Coherent many-body Rabi oscillations via superradiance and superabsorption and the mean-field approach for a superradiant laser

R. A. Dourado and M. H. Y. Moussa
Instituto de Física de São Carlos, Universidade de São Paulo, Caixa Postal 369, 13560-970, São Carlos, São Paulo, Brazil

(Received 5 March 2021; revised 16 July 2021; accepted 2 August 2021; published 17 August 2021)

The experimental success achieved in recent decades in the coherent manipulation of several Rabi cycles has led to a new stage in the physics of radiation-matter interaction. Motivated by this perspective, we propose here the engineering of coherent many-body Rabi oscillations (CMBROs) induced from the interactions of a moderately dense atomic sample with the environment and a high-finesse cavity mode. The CMBRO follows from the interplay between superradiance and superabsorption: the collective decay and absorption of the atomic sample inside the cavity. The equations we have derived for this interplay, based on the mean-field approximation, describe a two-level superradiant laser in an appropriate parameter regime, and its properties are also discussed. The control of quantum coherence according to the method presented here can be adapted to the implementation of quantum information processes as well as for the investigation of the fundamentals of quantum mechanics.

DOI: 10.1103/PhysRevA.104.023708

I. INTRODUCTION

The great experimental advance that has happened in the physics of radiation-matter interaction since the 1990s is mainly due to the strong electrical dipole couplings achieved together with the long lifetimes of the field (confined in high-finesse cavities) and the atomic Rydberg states. These ingredients combined together made it possible to manipulate high-fidelity states over relatively large timescales, especially in the fields of cavity quantum electrodynamics and trapped ions [1,2]. Much has been achieved within the possibilities offered by this time gap where several cycles of Rabi oscillations could be observed. We mention in particular the experimental demonstration of fundamental phenomena of quantum mechanics, as well as the implementation of quantum information processing, paving the way for the current status of quantum information theory [3], which essentially relies on the manipulation of quantum coherence.

In parallel with the development in the manipulation of the quantum states of a few two-level atoms and photons, there has also been a no less remarkable advance in the manipulation of many-body cold-atom states, such as the atomic Bose-Einstein condensates [4]. Here, the manipulation of quantum coherence has been extended to matter-wave states, enabling many interesting achievements [5]. More recently, to complete a chapter opened in 1954 with the theoretical prediction of superradiance by Dicke [6], in 2014 Higgins *et al.* [7] proposed the superabsorption of light, the reciprocal process to superradiance.

Our goal in this paper concerns the possibility of observing coherent many-body Rabi oscillations (CMBROs) through the interplay between superradiance and superabsorption. A moderately dense atomic excited sample, confined to a high-finesse cavity, is made to superradiate to a cavity mode and then to superabsorb the field back, repeating the process for several cycles. Evidently, we seek for a shorter period of emission and reabsorption in terms of the collective effects of both processes, which could, in principle, be used as an instrument to manipulate quantum coherence.

CMBRO has long been investigated [8] and has been studied since the early 2000s for a bold proposal to implement quantum processing in mesoscopic atomic ensembles [9]. These oscillations have been pursued on different experimental platforms, such as cold atoms [10], where these oscillations have already been observed [11]. Theoretical investigations also consider the emergence of CMBROs through interacting atoms in quantum liquid tubes [12]. In the present proposal we consider the interaction of an atomic sample with the environment and a high-finesse cavity mode. Instead of the emergence of the CMBROs from excitation blockage [9,11] or quantum quench [12], here, they must result from the interplay between superradiance and superabsorption phenomena. The equations derived for this interplay also describe a superradiant laser whose properties are discussed here.

This paper is organized as follows. In Sec. II we obtain the nonlinear mean-field Hamiltonian for the representative atom-field pair describing the process. In Sec. III, we obtain a system of coupled differential equations for the evolution of the expected values of the atomic and field operators. The complementary intensities of the emitted and reabsorbed radiation are also presented in Sec. III. The characterizations of superradiance and superabsorption are discussed in Sec. IV. In Sec. V we derive the mean-field equations for a two-level superradiant laser from the equations for the interplay between superradiant and superabsorption. In Sec. VI we present our conclusions.

II. THE NONLINEAR MEAN-FIELD HAMILTONIAN

We start with the Hamiltonian describing the process, $H = H_0 + H_I$, where

$$H_0 = \omega_0 a^\dagger a + \omega_0 S_z + \sum_k \omega_k b_k^\dagger b_k, \tag{1a}$$

$$H_I = g(aS_+ + a^\dagger S_-) + \sum_k \lambda_k (S_- b_k^\dagger + S_+ b_k). \tag{1b}$$

The diagonal operator H_0 accounts for the cavity mode ω_0, the atomic sample ω_0, and its reservoir ω_k. The cavity mode is assumed to be an ideal system, described by the creation operator $a^\dagger$ and annihilation operator a; the atomic sample is described by the collective pseudospin operator $S_z = \sum_{n=1}^{N} \sigma_z^{(n)}/2$, and the reservoir is a sample of harmonic modes described by the creation operator $b_k^\dagger$ and the annihilation operator b_k. The nondiagonal H_I refers to both the interactions shared by the atomic sample, with the reservoir λ_k and the cavity mode g, the latter being described by the Tavis-Cummings model, with the collective operators $S_\pm = \sum_{n=1}^{N} \sigma_\pm^{(n)}$. Going to the interaction picture where

$$\mathcal{H}_I(t) = g(aS_+ + a^\dagger S_-) + \sum_k \lambda_k (S_- b_k^\dagger e^{i(\omega_k - \omega_0)t} + S_+ b_k e^{-i(\omega_k - \omega_0)t}) \tag{2}$$

and tracing out the reservoir variables, we obtain the master equation governing the evolution of the atom-field state

$$\dot{\rho}(t) = -i[\,\omega_0 a^\dagger a + \omega_0 S_z + g(aS_+ + a^\dagger S_-),\, \rho(t)] + \mathcal{L}\rho(t), \tag{3}$$

where the Lindbladian form

$$\mathcal{L}\rho(t) = \gamma_{21}[2S_-\rho(t)S_+ - S_+S_-\rho(t) - \rho(t)S_+S_-] - \gamma_{12}[2S_+\rho(t)S_- - S_-S_+\rho(t) - \rho(t)S_-S_+], \tag{4}$$

with $\gamma_{21} = \gamma(\bar{n}+1)/2$ and $\gamma_{12} = \gamma\bar{n}/2$, is a signature of the superradiance phenomena, the collective spontaneous emission of light of a moderately dense atomic sample in an initially inverted populated state, with γ being the atomic relaxation factor and $\bar{n}$ being the mean excitation of the reservoir modes.

In order to apply the mean-field approximation [13,14], we take advantage of the canonical mapping [15]

$$a \to \frac{1}{\sqrt{N}} \sum_{i=1}^{N} a_i, \quad a^\dagger a \to \sum_{i=1}^{N} a_i^\dagger a_i, \tag{5}$$

which introduces N mathematical cavity modes in place of the single physical one, thus helping us to describe the system through a single representative atom-field pair. Equation (5) enables us to rewrite the atom-field Hamiltonian, in the von Neumann term of the master equation (3), as

$$\mathcal{H} = \omega_0 \sum_{i=1}^{N} \left(a_i^\dagger a_i + \frac{\sigma_z^{(i)}}{2} \right) + \frac{\tilde{g}}{N} \sum_{i \neq j=1}^{N} (a_i \sigma_+^j + a_i^\dagger \sigma_-^j), \tag{6}$$

where the atom-field coupling scales to $\tilde{g} = g\sqrt{N}$. Assuming that the density operators for the atomic sample and the cavity modes are initially factorized, the mean-field approximation follows by tracing out all the $N-1$ atom-field pairs except for the representative one, leading, in the limit of an infinite number of pairs, to [16]

$$\lim_{N\to\infty} \mathrm{Tr}_2 \cdots \mathrm{Tr}_N\, [\mathcal{H}, \rho_N(t)] = \left[\omega_0 \left(a^\dagger a + \frac{\sigma_z}{2} \right), \rho_{AF}(t) \right] + \lim_{N\to\infty} \frac{N-1}{N} \tilde{g}\, \mathrm{Tr}_2 \left[\sum_{i\neq j=1}^{2} (a_i \sigma_+^j + a_i^\dagger \sigma_-^j), \rho_2(t) \right], \tag{7}$$

where $\rho_{AF}(t)$ stands for the representative atom-field pair. Assuming, in addition, the *uncorrelated approximation*, by which we disregard the statistical correlations in the two-body operator, factorizing it as the product of two one-body operators, i.e., $\rho_2(t) = \rho_{AF}(t) \otimes \rho_{AF}(t)$ [17], we end up with the nonlinear master equation

$$\dot{\rho}_{AF}(t) = -i\left[\omega_0 \left(a^\dagger a + \frac{\sigma_z}{2} \right) + \tilde{g}(a\langle\sigma_+\rangle + \langle a\rangle\sigma_+ + a^\dagger\langle\sigma_-\rangle + \langle a^\dagger\rangle\sigma_-), \rho_{AF}(t) \right] + \mathrm{Tr}_2 \cdots \mathrm{Tr}_N\, \mathcal{L}\rho(t). \tag{8}$$

Next, by also tracing out the $N-1$ atom-field pairs engaged in the interaction of the atomic sample with the environment, we finally obtain

$$\dot{\rho}_{AF} = -i[H_{AF}, \rho_{AF}] + \gamma_{21}(2\sigma_-\rho_{AF}\sigma_+ - \sigma_+\sigma_-\rho_{AF} - \rho_{AF}\sigma_+\sigma_-) + \gamma_{12}(2\sigma_+\rho_{AF}\sigma_- - \sigma_-\sigma_+\rho_{AF} - \rho_{AF}\sigma_-\sigma_+), \tag{9}$$

where the nonlinear mean-field Hamiltonian in the von Neumann term of Eq. (8), which accounts for the representative atom-field pair, is changed to

$$H_{AF} = \omega_0 \left(a^\dagger a + \frac{\sigma_z}{2} \right) + \sqrt{N} g \left(\langle\sigma_+\rangle a + \langle\sigma_-\rangle a^\dagger \right) + \Lambda \langle\sigma_-\rangle \sigma_+ + \Lambda^* \langle\sigma_+\rangle \sigma_-, \tag{10}$$

where

$$\Lambda = \frac{N}{2} \left(\frac{2g}{\sqrt{N}} \frac{\langle a \rangle}{\langle \sigma_- \rangle} - i\gamma \right) = |\Lambda|\, e^{i\phi_\Lambda}, \tag{11a}$$

$$|\Lambda| = \sqrt{N} \left[\left(g\cos(\phi_a - \phi_{\sigma_-}) \frac{|\langle a\rangle|}{|\langle\sigma_-\rangle|} \right)^2 + \left(g\sin(\phi_a - \phi_{\sigma_-}) \frac{|\langle a\rangle|}{|\langle\sigma_-\rangle|} - \frac{\sqrt{N}}{2}\gamma \right)^2 \right]^{1/2}, \tag{11b}$$

$$\phi_\Lambda = \tan^{-1} \left(\frac{2g\sin(\phi_a - \phi_{\sigma_-})|\langle a\rangle| - \gamma\sqrt{N}|\langle\sigma_-\rangle|}{2g\cos(\phi_a - \phi_{\sigma_-})|\langle a\rangle|} \right). \tag{11c}$$

In what follows we disregard the superoperators in Eq. (9) taking into account the atomic dissipative and absorptive terms since we will be interested in much shorter time intervals than the relaxation time γ^{-1}.

III. EXPECTED VALUES

We next present a system of coupled differential equations for the evolution of the expected values of the atomic and field operators. After defining the relations $\langle a\rangle = \langle a^\dagger\rangle^* = |\langle a\rangle|e^{i\phi_a}$ and $\langle\sigma_-\rangle = \langle\sigma_+\rangle^* = |\langle\sigma_-\rangle|e^{i\phi_\sigma}$, we obtain

$$\begin{aligned}\dot{\langle\sigma_z\rangle} &= -4\sqrt{N}g\sin(\phi_\sigma-\phi_a)|\langle a\rangle||\langle\sigma_-\rangle| - 2N\gamma|\langle\sigma_-\rangle|^2\\ &= 4|\Lambda|\sin\phi_\Lambda|\langle\sigma_-\rangle|^2 \qquad (12a)\end{aligned}$$

$$|\dot{\langle\sigma_-\rangle}| = -\sqrt{N}g\sin(\phi_a-\phi_\sigma)|\langle a\rangle||\langle\sigma_z\rangle| + \frac{N\gamma}{2}|\langle\sigma_-\rangle|, \qquad (12b)$$

$$\dot{\langle a^\dagger a\rangle} = 2\sqrt{N}g\sin(\phi_\sigma-\phi_a)|\langle a\rangle||\langle\sigma_-\rangle|, \qquad (12c)$$

$$|\dot{\langle a\rangle}| = \sqrt{N}g\sin(\phi_\sigma-\phi_a)|\langle\sigma_-\rangle|, \qquad (12d)$$

$$\dot{\phi_{\sigma_-}} = -\omega_0 + \sqrt{N}g\cos(\phi_\sigma-\phi_a)\frac{|\langle a\rangle|}{|\langle\sigma_-\rangle|}\langle\sigma_z\rangle, \qquad (12e)$$

$$\dot{\phi_a} = -\omega_0 - \sqrt{N}g\cos(\phi_\sigma-\phi_a)\frac{|\langle\sigma_-\rangle|}{|\langle a\rangle|}. \qquad (12f)$$

Moreover, from the energies of the representative atom and field mode, given by $\epsilon_A = \omega_0\langle\sigma_z\rangle/2$ and $\epsilon_F = \omega_0\langle a^\dagger a\rangle$, we obtain the complementary intensities for the emitted and reabsorbed radiation:

$$\begin{aligned}\mathcal{I}_A &= -N\frac{d\epsilon_A}{dt} = N\omega_0|\langle\sigma_-\rangle|[N\gamma|\langle\sigma_-\rangle|\\ &\quad +2\sqrt{N}g\sin(\phi_\sigma-\phi_a)|\langle a\rangle|], \qquad (13a)\\ \mathcal{I}_F &= -N\frac{d\epsilon_F}{dt} = -2N^{3/2}g\omega_0\sin(\phi_\sigma-\phi_a)|\langle a\rangle||\langle\sigma_-\rangle|\\ &= N^2\gamma\omega_0|\langle\sigma_-\rangle|^2 - \mathcal{I}_A, \qquad (13b)\end{aligned}$$

In the above complementary equations, the photons resulting from the superradiance of the atomic sample ($\mathcal{I}_A > 0$) are stored by the cavity field ($\mathcal{I}_F < 0$) and then superabsorbed back by the sample ($\mathcal{I}_A < 0$) when the cavity field is emptied to restart a new cycle. Equations (13) for the complementary intensities (the interplay between superradiance and superabsorption) have a very distinctive feature when compared to those in which the processes of superradiance and superabsorption are independent of each other, both being described by the expression $N^2\gamma\omega_0|\langle\sigma_-\rangle|^2$. The distinctive feature is the contribution of the term $2N^{3/2}g\omega_0\sin(\phi_\sigma-\phi_a)|\langle a\rangle||\langle\sigma_-\rangle|$, which in the interplay causes the intensities $\mathcal{I}_A$ and $\mathcal{I}_F$ to exceed those of the independent processes. In short, in the interplay between superradiance and superabsorption, one process strengthens the other, both in terms of the peak of their intensities and in terms of their frequencies, which, as we will see below, are greater than those in which the processes occur separately.

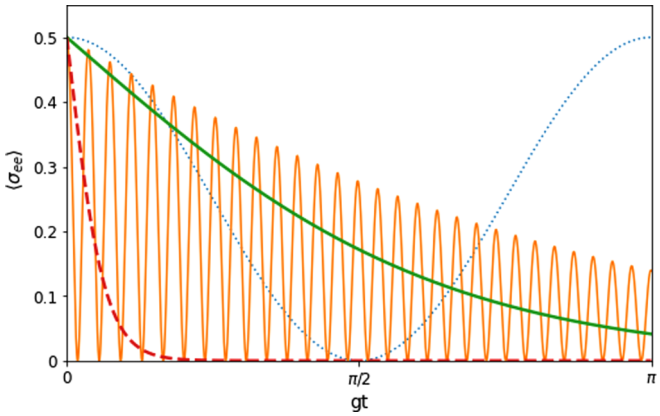

FIG. 1. Mean population $\langle\sigma_+\sigma_-\rangle$ against gt for $N = 1$ (dotted blue line) and $N = 10^3$ (solid orange line). We also have $\langle\sigma_+\sigma_-\rangle$ for an atomic sample undergoing the usual superradiant decay ($g = 0$; thick solid green line) and the decay for an engineered reservoir (thick dashed red line).

IV. CHARACTERIZATIONS OF SUPERRADIANCE AND SUPERABSORPTION

The superradiance and superabsorption mechanisms follow from the nondiagonal terms of the nonlinear Hamiltonian (10). When disregarding the interaction of the atomic sample with the cavity mode ($g = 0$), leaving only superradiance, the frequency (11a) reduces to $\Lambda = iN\gamma/2$ (where $\gamma = \gamma_{21} - \gamma_{12}$), and consequently, $\dot{\langle\sigma_z\rangle} = -2N\gamma|\langle\sigma_-\rangle|^2$. On the other side, when considering only the superabsorption mechanism, by which the atomic sample is subjected to the collective absorption described by the Lindbladian in Eq. (4), with $\gamma = \gamma_{12} - \gamma_{21}$, we get $\dot{\langle\sigma_z\rangle} = 2N\gamma|\langle\sigma_-\rangle|^2$. Therefore, the difference between superradiance and superabsorption is, as expected, the signal of $\dot{\langle\sigma_z\rangle}$; while the atomic population decreases in superradiance, it grows in superabsorption. From Eq. (12a), we verify that the time-dependent sine function automatically takes into account both signals of $\dot{\langle\sigma_z\rangle}$, leading to superradiance when $\pi < \phi_\Lambda < 2\pi$, and superabsorption when $0 < \phi_\Lambda < \pi$. In our interplay, however, instead of the usual Lindbladian for collective absorption, the superabsorption process is triggered by the cavity mode that feeds back the atomic sample through an effective coupling enhanced by a factor $\sqrt{N}$.

To illustrate the CMBROs, we start with the field in the vacuum state and the atom in the superposition $\cos\theta|e\rangle + \sin\theta e^{i\phi_\sigma(0)}|g\rangle$, with $\theta = \pi/2$ and $\phi_\sigma(0) = 0$, to plot in Fig. 1, against gt, the mean population of the atomic excited state $\langle\sigma_+\sigma_-\rangle$ for $N = 1$ (dotted blue line) and $N = 10^3$ (solid orange line), using, in units of g from here on, $\omega_0 = 10^2$ and $\gamma = 10^{-3}$. We also plot in Fig. 1 the mean population $\langle\sigma_+\sigma_-\rangle$ for an atomic sample, with $N = 10^3$ and $\gamma = 10^{-3}$, undergoing the usual superradiant decay ($g = 0$) (thick solid green line) and for an engineered reservoir [18], where the decay rate is changed to $g^2/\kappa > \gamma$ (thick dashed red line), with $\kappa = 10^2$ being the decay rate of a bad cavity into which the atomic sample is placed.

We thus clearly observe in Fig. 1 the CMBRO, the interplay between superradiance and superabsorption, one strengthening the other, with the time of collective decay and absorption

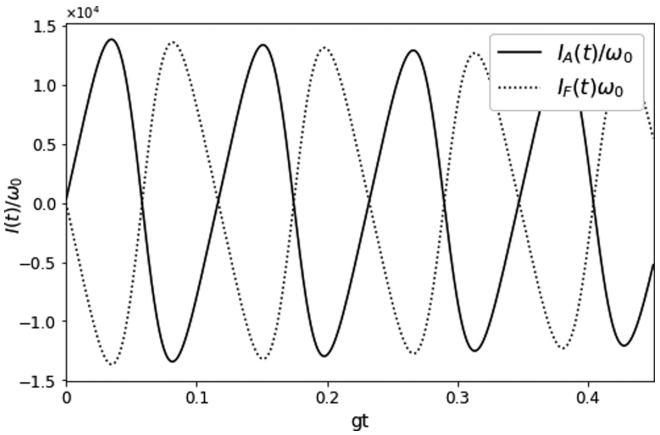

FIG. 2. Intensities $\mathcal{I}_A/\omega_0$ and $\mathcal{I}_F/\omega_0$ against gt when $\gamma_{12} < \gamma_{21}$.

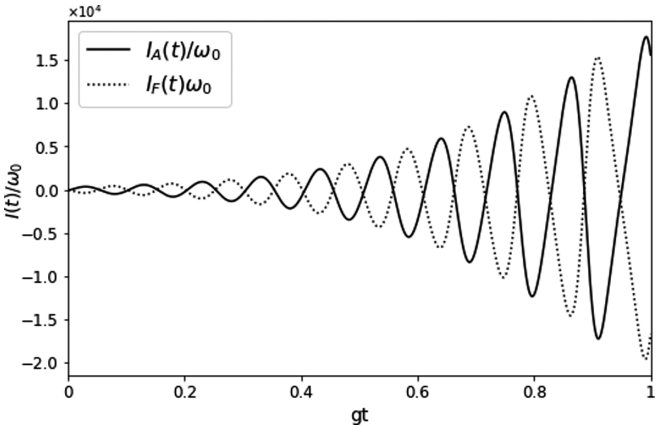

FIG. 3. Intensities $\mathcal{I}_A/\omega_0$ and $\mathcal{I}_F/\omega_0$ against gt under the multimodal amplification of the atomic sample, such that $\gamma_{12} > \gamma_{21}$.

being even shorter than that of the superradiant decay for an engineered reservoir (coming from the thick dashed line). We have already pointed out that the intensities of superradiance and superabsorption when interplaying with each other can surpass those of the independent processes. To illustrate this, in Fig. 2 we plot the intensities $\mathcal{I}_A/\omega_0$ and $\mathcal{I}_F/\omega_0$ against gt, given by the solid and dotted lines, respectively, using $N = 10^3$ and the same initial states and parameter γ as in Fig. 1. The complementary curves show that there is an average frequency for superradiance and superabsorption, associated with the time of collective decay and absorption, around $10^{-1}g$ for the parameters we have used. Regarding the maximum height of the curves, they are slightly above the value $N^2\gamma|\langle\sigma_-\rangle|^2 = 125$, taking into account that the maximum value of $|\langle\sigma_-\rangle|$ is 1/2.

V. FROM THE INTERPLAY BETWEEN SUPERRADIANCE AND SUPERABSORPTION TO THE MEAN-FIELD EQUATIONS FOR A TWO-LEVEL SUPERRADIANT LASER

To derive the mean-field laser theory we next consider the interplay of superradiance and superabsorption in a modified version of the mean-field master equation (9). We must introduce in this mean-field equation the Lindbladian for the cavity decay $\kappa_{21}(2a\rho_{AF}a^\dagger - a^\dagger a\rho_{AF} - \rho_{AF}a^\dagger a)$ and also a multimodal amplification, the reciprocal of the reservoir [19], that takes the atoms from the ground to the excited state, making the absorption rate higher than the emission rate: $\gamma_{12} > \gamma_{21}$. We are proposing here a two-level superradiant laser, from which the usual nonlasing fundamental level is absent. By defining $A(t) = \langle a(t)\rangle e^{i\omega t}$, $S(t) = \langle\sigma_-(t)\rangle e^{i\omega t}$, $D(t) = \langle\sigma_z(t)\rangle$, $\tilde{g} = ig$, $\Gamma = (\gamma_{12} + \gamma_{21})/2$, and $d = (\gamma_{12} - \gamma_{21})/2\Gamma$, we end up with the nonlinear system

$$\frac{dA}{dt} = -\kappa A - \sqrt{N}\tilde{g}AD, \tag{14a}$$

$$\frac{dS}{dt} = -\Gamma[1 + d(N-1)D]S + \sqrt{N}\tilde{g}AD, \tag{14b}$$

$$\frac{dD}{dt} = 2\sqrt{N}\tilde{g}[A^*S - AS^*] - 2\Gamma[D - d] + 4d(N-1)\Gamma|S|^2, \tag{14c}$$

which must be analyzed in two different regimes: the interplay regime for $\Gamma \ll \sqrt{N}g$ and the superradiant laser for $\Gamma \gg \sqrt{N}g$. In the above equations the transition $g \to e$ occurs by superabsortion (rate $dN\Gamma$) and incoherent excitation (rate Γ), both coming from the multimodal amplification. In turn, the transition $e \to g$ occurs by superradiance (rate $\sqrt{N}g$). When considering $N = 1$, the system (14) reduces exactly to the mean-field equations of the usual laser theory [15].

Starting with the interplay regime, we consider the field in the vacuum state and the atom in the superposition $\cos\theta|e\rangle + \sin\theta e^{i\phi_\sigma(0)}|g\rangle$, now with $\theta = \pi/2 - 20/N$ and $\phi_\sigma(0) = 0$. Using the same parameters as in Fig. 2, except for $\gamma = -10^{-2}$, we then plot in Fig. 3 the intensities $\mathcal{I}_A$ and $\mathcal{I}_F$ (solid and dotted lines, respectively), showing again the interplay between superradiance and superabsorption, but now with both intensities increasing over time due to the multimodal amplification of the atomic sample.

Turning now to the laser regime, we first observe that when considering $N = 1$, the system (14) reduces exactly to the mean-field equations of the usual laser theory [15], where the relation $\Gamma \gg g \gg \kappa$ enable us to eliminate the fast variables S and D, leading us to the equation for the field amplitude

$$\frac{dA}{dt} = -\kappa A\left(1 - \frac{C}{1 + |A|^2/n_0}\right), \tag{15}$$

where $C = dg^2/\Gamma\kappa$ is the laser pump parameter and $n_0 = \Gamma^2/2g^2$. As shown in Fig. 4, where we consider $\Gamma = 10$ and $\kappa = 10^{-2}$, at $C = 1$ we have a threshold between a unique stationary solution $A = 0$ ($C < 1$) and a region ($C > 1$) where this vacuum solution becomes unstable (dashed line), thus enabling us to excite the cavity field to the stationary solutions $|A|^2 = n_0(C - 1)$ (solid line).

Considering now our superradiant laser, we observe that by increasing N the threshold moves to smaller values of C, as shown in Fig. 5, where we consider $N = 5$ and the same parameters used in Fig. 4, indicating that the collective effects of superradiance demand a smaller pump parameter to establish the laser phase transition. Remarkably, the collective effects of our superradiant laser dispense the need for a field pumping

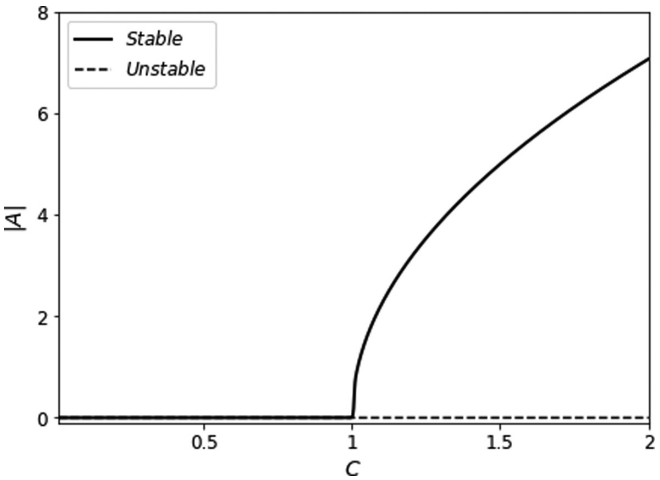

FIG. 4. Bifurcation diagram for the field amplitude of a usual laser ($N = 1$) coming from Eq. (15), with $\Gamma = 10$ and $\kappa = 10^{-2}$.

rate higher than that of damping for the establishment of the laser regime.

Another interesting issue coming from the collective effects of the superradiant laser, again with $N = 5$, is the double-threshold transitions shown in Fig. 6, owing to a different choice of parameters: $\Gamma = 10$ and $\kappa = 10^{-1}$. Now we have a threshold towards the laser field for C between 0.2 and 0.3 and a threshold out of the laser field at $C = 1$. The dashed line indicates the unstable vacuum solution.

Next, ensuring that the system is above the threshold by setting the parameters $\Gamma = 10$ and $\kappa = 10^{-1}$, we then solve the system (14) to compute the intensity of the cavity field, $\mathcal{I}_F = Nd\epsilon_F/dt$, now taking into account the dissipative terms in Eq. (9), different from what was done in the derivation of Eq. (13b), where we were interested in time intervals much shorter than γ^{-1}. Now we are evidently interested in the steady-state regime, where the competition between amplification and dissipation, mediated by saturation, plays a fundamental role. In Fig. 7 we plot the intensities for $N = 1, 5,$

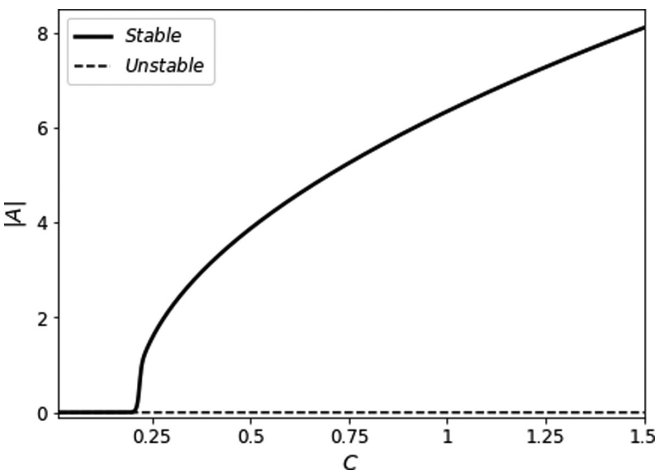

FIG. 5. Bifurcation diagram for the field amplitude of our superradiant laser ($N = 5$) coming from Eq. (14), with the same parameters used in Fig. 4.

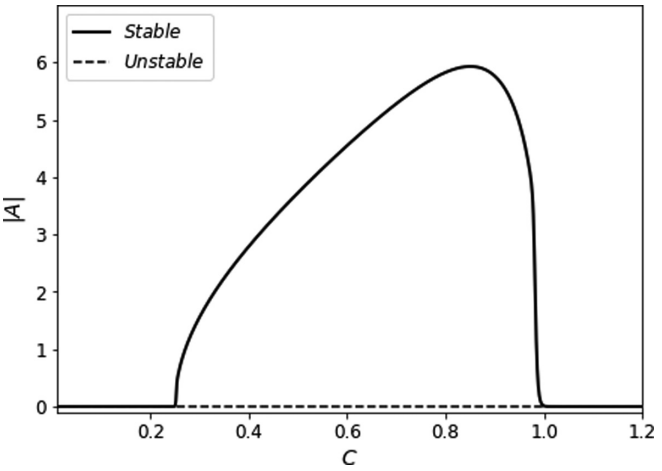

FIG. 6. Bifurcation diagram for the field amplitude of our superradiant laser ($N = 5$) coming from Eq. (14), with $\Gamma = 10$ and $\kappa = 10^{-1}$.

and 10, using the same parameters as in Fig. 4 with $d = 0.8$, showing that their maxima grow as N^2, a scale law that is better the higher N is, similar to the superradiant laser in Ref. [20], another interesting feature of our laser.

Finally, we analyze the laser linewidth coming from the second-order correlation function $\langle E^-(t)E^+(t+\tau)\rangle \approx \langle E^+(\tau)\rangle = |A|^2 e^{-i\omega_0\tau}e^{-D\tau}$:

$$L(\omega) = \frac{|A|^2}{\pi}\frac{D}{(\omega-\omega_0)^2 + D^2},$$

with both diffusion D and the mean number of photons $|A|^2$ being numerically computed. The linewidth is plotted in Fig. 8 for $N = 1$, 5, and 20 using the same parameters as in Fig. 7, showing, interestingly, that it is not much affected by N.

VI. CONCLUSIONS

Considering a moderately dense atomic sample inside a high-finesse cavity, we demonstrated the possibility of building an interplay between superradiance and superabsorption

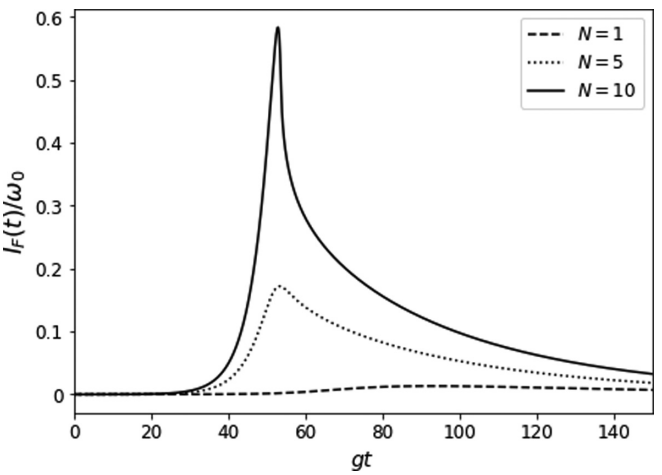

FIG. 7. Intensities against gt for $N = 1$, 5, and 10.

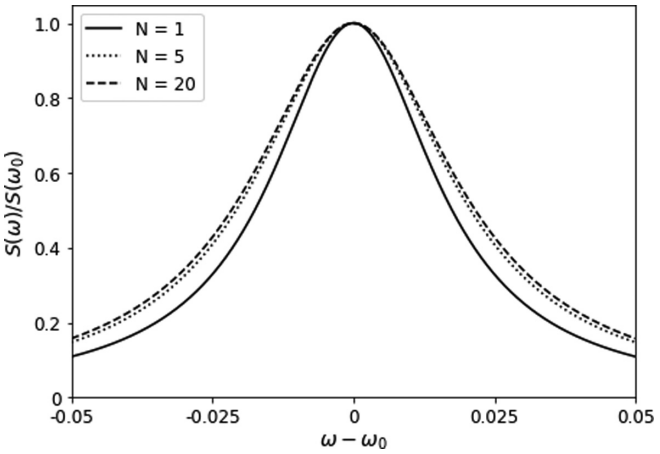

FIG. 8. Linewidth against gt for $N = 1$, 5, and 20.

that leads to CMBROs. While the superradiance is triggered, as usual, by the atomic sample reservoir, transferring the atomic excitation to the cavity mode, the superabsorption of that excitation back to the sample results from a Rabi frequency increased by the factor $\sqrt{N}$. The first notable feature is that in the interplay, superradiance and superabsorption cooperate, strengthening each other, shortening their typical emission and absorption times and increasing their intensities.

In addition to the interplay between superradiance and superabsorption, we also showed a regime leading to a two-level superradiant laser whose intensity scales as N^2 and whose linewidth is roughly the same as that of the conventional laser ($N = 1$).

ACKNOWLEDGMENTS

The authors would like to thank CAPES and INCT-IQ for support.

The authors declare no conflicts of interest.

[1] S. Haroche, Rev. Mod. Phys. **85**, 1083 (2013).
[2] D. J. Wineland, Rev. Mod. Phys. **85**, 1103 (2013).
[3] M. A. Nielsen and I. L. Chuang, *Quantum Computation and Quantum Information* (Cambridge University Press, Cambridge, 2010).
[4] W. Ketterle, Rev. Mod. Phys. **74**, 1131 (2002); E. A. Cornell and C. E. Wieman, *ibid.* **74**, 875 (2002).
[5] K. Bongs and K. Sengstock, Rep. Prog. Phys. **67**, 907 (2004).
[6] R. H. Dicke, Phys. Rev. **93**, 99 (1954).
[7] K. D. B. Higgins, S. C. Benjamin, T. M. Stace, G. J. Milburn, B. W. Lovett, and E. M. Gauger, Nat. Commun. **5**, 4705 (2014).
[8] E. R. Buley and F. W. Cummings, Phys. Rev. **134**, A1454 (1964); F. W. Cummings and A. Dorri, Phys. Rev. A **28**, 2282 (1983).
[9] M. D. Lukin, M. Fleischhauer, R. Cote, L. M. Duan, D. Jaksch, J. I. Cirac, and P. Zoller, Phys. Rev. Lett. **87**, 037901 (2001).
[10] S. Stanojevic and R. Coté, Phys. Rev. A **80**, 033418 (2009).
[11] Y. O. Dudin, L. Li, F. Bariani, and A. Kuzmich, Nat. Phys. **8**, 790 (2012).
[12] S. D. Huber and E. Altman, Phys. Rev. Lett. **103**, 160402 (2009).
[13] G. S. Agarwal, *Quantum Statistical Theories of Spontaneous Emission*, Springer Tracts in Modern Physics Vol. 70 (Springer, Berlin, 1984).
[14] S. S. Mizrahi, Phys. Lett. A **144**, 282 (1990); S. S. Mizrahi and M. A. Mewes, Int. J. Mod. Phys. B **7**, 2353 (1993).
[15] H. P. Breuer and F. Petruccione, *The Theory of Open Quantum Systems* (Oxford University Press, Oxford, 2002).
[16] H. Spohn, Rev. Mod. Phys. **52**, 569 (1980).
[17] G. S. Agarwal, Phys. Rev. A **4**, 1791 (1971).
[18] V. V. Temnov and U. Woggon, Phys. Rev. Lett. **95**, 243602 (2005).
[19] Superabsorption may be achieved by considering a multimodal amplification of a moderately dense atomic sample, whose frequency of transition ω_0 leads to a wavelength $2\pi c/\omega_0$ greater than the size of the sample. This can be done by transposing to an atomic sample the arguments developed for a network of dissipative oscillators presented by M. A. de Ponte, S. S. Mizrahi, and M. H. Y. Moussa Phys. Rev. A **76**, 032101 (2007). This consideration was not necessary for the case $\gamma_{12} < \gamma_{21}$, where the enhanced coupling of the atomic sample with the cavity mode accounts for the superabsorption.
[20] F. Haake, M. I. Kolobov, C. Fabre, E. Giacobino, and S. Reynaud, Phys. Rev. Lett. **71**, 995 (1993).